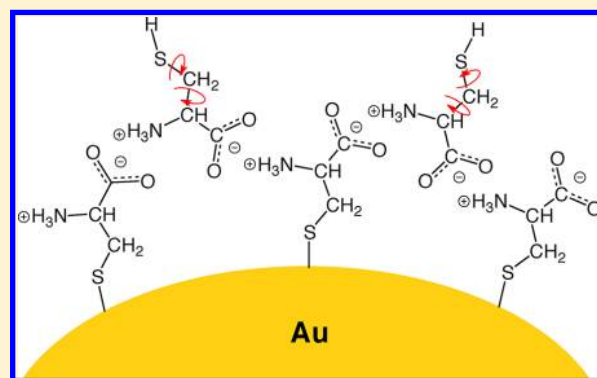


# $^1\text{H}$ MAS NMR Study of Cysteine-Coated Gold Nanoparticles

Anuji Abraham,<sup>†</sup> Andrew J. Illott,<sup>‡</sup> Joel Miller,<sup>§</sup> and Terry Gullion<sup>\*,†</sup><sup>†</sup>Department of Chemistry, West Virginia University, Morgantown, West Virginia 26506, United States<sup>‡</sup>Department of Chemistry, SUNY Stony Brook, Stony Brook, New York 11794, United States<sup>§</sup>Chemistry Division, Naval Research Laboratory, Code 6122, Washington, DC 20375, United States

## S Supporting Information

**ABSTRACT:**  $^1\text{H}$  MAS NMR experiments were performed on gold nanoparticles coated with L-cysteine. The experiments show that L-cysteine molecules are zwitterions and support a structural model of cysteine forming two layers. The inner layer is composed of cysteine molecules chemisorbed to the gold surface via the sulfur atom. The outer layer interacts with the chemisorbed layer. The  $^1\text{H}$  NMR suggests that the cysteine in the outer layer exhibits large amplitude motion about specific carbon–carbon bonds.



## INTRODUCTION

Cysteine can bind to gold via the thiol group, with concomitant loss of the  $-\text{SH}$  proton, either in its molecular form or as part of a peptide.<sup>1,2</sup> Adsorption of L-cysteine onto gold surfaces under various conditions has been studied using a variety of techniques, and different adsorption modes are observed in the solid phase. Dimers, self-assembled monolayers and double layer features have been observed under ultrahigh vacuum conditions using well-defined Au (111) and Au (110) surfaces.<sup>3–10</sup> Likewise, monolayers have been observed and double layer models proposed for samples using solution phase adsorption of cysteine on gold electrodes and surfaces.<sup>11–16</sup> Only a few of the aforementioned results report double layer coverage of the gold surfaces,<sup>8,9,12,13</sup> and none of the experiments were on gold nanoparticles. Since a wide variety of cysteine structures have been observed on well-defined gold surfaces, and because of the current interest in biological applications of nanoparticles, then it is desirable to study the structure of cysteine and other biological molecules on gold nanoparticles.

Recent  $^{13}\text{C}$  and  $^{15}\text{N}$  MAS NMR (magic-angle spinning nuclear magnetic resonance) experiments at ambient conditions on gold nanoparticles coated with uniformly  $^{13}\text{C}$  and  $^{15}\text{N}$  labeled L-cysteine show the presence of two types of cysteine for solid phase samples.<sup>17</sup> A structural model of the system from the NMR study shows that one type of cysteine forms a layer chemisorbed to the gold surface via the sulfur atom and the other type of cysteine forms an outer layer to the chemisorbed layer. Stabilization of the two-layer structure presumably occurs via intermolecular hydrogen bonding between charged amino and carboxylate groups of the zwitterions. In this model the outer layer would have

protonated thiol groups oriented away from the gold surface. This NMR-based structural model of nanoparticles is in accord with structures put forth by metastable deexcitation spectroscopy<sup>8</sup> and X-ray photoelectron spectroscopy<sup>10</sup> studies of cysteine deposited on well-defined gold surfaces under ultrahigh vacuum conditions.

The evidence for two species of cysteine in the gold nanoparticle system is from the observed  $^{13}\text{C}$  and  $^{15}\text{N}$  isotropic chemical shift positions in MAS NMR experiments and from thermogravimetric experiments.<sup>17</sup> A pair of  $^{13}\text{C}$  resonances for each of the  $\text{C}_2$  and  $\text{C}_3$  carbons is observed. Each  $\text{C}_2$  and  $\text{C}_3$  carbon has a  $^{13}\text{C}$  resonance located near their respective positions observed for polycrystalline cysteine and a resonance deshielded by approximately 12 ppm. The set of deshielded resonances is attributed to chemisorbed cysteine molecules, and the other set of resonances is assigned to cysteine molecules forming an outer layer to the chemisorbed layer. Contrarily, only a single  $^{13}\text{C}$  resonance is observed for the  $\text{C}_1$  carbon, and it is located near the position observed for crystalline cysteine. A single  $^{15}\text{N}$  resonance is observed for cysteine-coated gold nanoparticles, and its position is shifted only slightly from that observed for crystalline cysteine. Because the positions of the  $^{13}\text{C}$  resonance of the  $\text{C}_1$  carbon and the  $^{15}\text{N}$  resonance are similar to their observed positions for crystalline cysteine, it appears that the amino and carboxylate groups do not interact significantly with the gold surface. Thermogravimetric (TGA) experiments also show the presence of two types of cysteine, with one type coming off at 110  $^\circ\text{C}$  and the other type coming

Received: February 3, 2012

Revised: June 15, 2012

Published: June 18, 2012

off at 280 °C.<sup>17</sup> The TGA result shows the amounts of the two types of cysteine are close to being equal and is suggestive of a bilayer.

<sup>1</sup>H MAS NMR experiments performed on polycrystalline cysteine and on solid-phase cysteine-gold nanoparticles are described in this paper. The <sup>1</sup>H NMR results support a structural model having two layers of cysteine coating the gold and provide additional details about molecular dynamics of the cysteine in the outer layer that were not evident in an earlier <sup>13</sup>C NMR study. A <sup>1</sup>H resonance for the thiol proton is observed in the cysteine-gold nanoparticle sample, providing direct evidence that not all cysteine molecules are chemisorbed. The <sup>1</sup>H spectrum of the gold nanoparticle sample shows that the cysteine molecules are in zwitterionic form. In addition, the cysteine-gold nanoparticle system showed two sets of proton resonances; one set consisted of broad resonances and the other set was made of sharp resonances. We postulate that the set containing the broad <sup>1</sup>H resonances arises from chemisorbed cysteine molecules, and the set containing the sharp <sup>1</sup>H resonances comes from an outer layer of cysteine. Furthermore, the set of sharp <sup>1</sup>H NMR resonances provides evidence of large amplitude motions about specific carbon-carbon bonds of molecules in the outer layer.

## EXPERIMENTAL SECTION

**Sample Preparation.** Gold nanoparticles were coated with L-cysteine by a previously described method that produced 6.6 ± 2.7 nm diameter particles.<sup>17</sup> Cysteine-coated gold nanoparticle samples were prepared with [1-<sup>13</sup>C, 99 at. %] L-cysteine and are referred to as <sup>13</sup>C-CysAu. The <sup>13</sup>C labeled cysteine was purchased from Cambridge Isotope Laboratories, Inc. Briefly, 120 mL of 0.5 mM gold(III) chloride trihydrate solution was reduced with 0.015 g of sodium borohydride to produce a ruby red solution of gold nanoparticles. A total of 400 mL of 1 mM isotopically labeled L-cysteine solution was added to the gold nanoparticle solution. The solution was stirred for 30 min and then left standing overnight. The cysteine-coated nanoparticles were separated from solution by centrifugation at 20 000g for 30 min. The supernatant was removed and the nanoparticles were washed several times with water and then dried overnight at 333 K. Sample weights for the NMR measurements were approximately 1.5 mg.

In addition to the gold nanoparticle samples, solid-state NMR experiments were performed on <sup>13</sup>C labeled cysteine and on <sup>2</sup>H labeled cysteine. [1-<sup>13</sup>C, 99 at. %] L-cysteine was recrystallized from water and is referred to as <sup>13</sup>C-Cys. [3,3'-<sup>2</sup>H, 98 at. %] L-cysteine was purchased from Cambridge Isotope Laboratories, Inc. and recrystallized from D<sub>2</sub>O having a small amount of added HCl and is named <sup>2</sup>H-Cys.

**Solid-State NMR.** Two solid-state NMR spectrometers were used to generate the results presented in this paper.

The <sup>1</sup>H and <sup>2</sup>H NMR spectra in Figure 1 were obtained on a 9.4 T Varian Inova spectrometer with a proton frequency of 399.89 MHz using a 3.2 mm Varian/Chemagnetics T3 solid-state probe-head. The <sup>1</sup>H and <sup>2</sup>H 90° pulse lengths were 5.0 and 4.0 μs, respectively. Recycle delay times were 10 s. The spectrometer was located at the State University of New York at Stony Brook.

The spectra in Figures 2 and 4 were obtained on a Varian spectrometer located at the Naval Research Laboratory (Washington, DC). The proton operating frequency was 500.1765 MHz. A Varian 1.2 mm double-resonance solid-state NMR probe was used. The <sup>1</sup>H and <sup>13</sup>C 90° pulse lengths

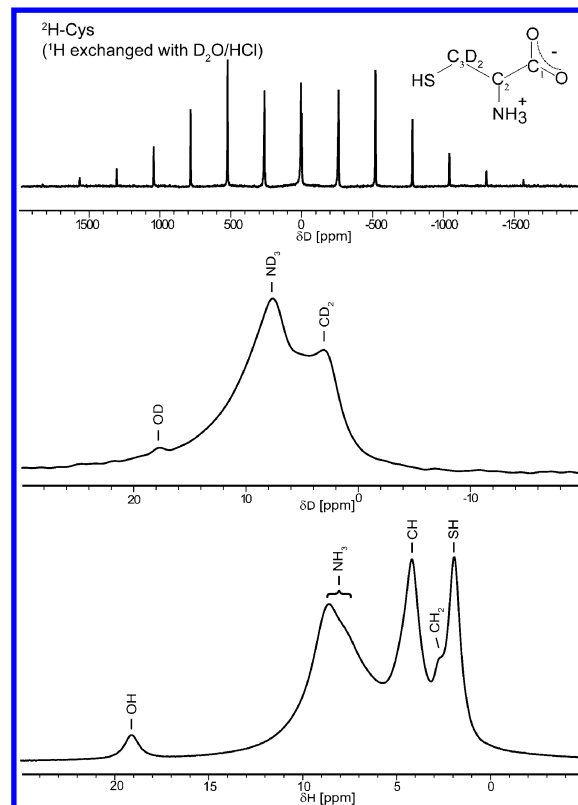


**Figure 1.** <sup>2</sup>H MAS NMR spectrum of <sup>2</sup>H-Cys is shown in the top spectrum. An expansion of the centerband of the <sup>2</sup>H MAS NMR spectrum with peak assignments is shown in the middle spectrum. The <sup>1</sup>H MAS NMR spectrum of <sup>2</sup>H-Cys is shown in the bottom spectrum along with peak assignments. Sixty-four transients were taken for each of the <sup>2</sup>H and <sup>1</sup>H spectra. All spectra were obtained with a MAS spinning speed of 18 kHz.

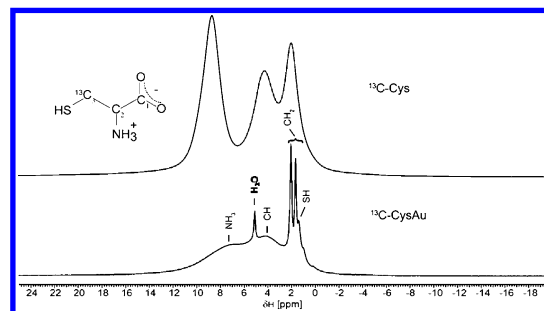


**Figure 2.** <sup>1</sup>H MAS NMR spectrum of <sup>13</sup>C-Cys is shown in the top spectrum. The <sup>1</sup>H resonances for the -NH<sub>3</sub><sup>+</sup>, -CH, and -CH<sub>2</sub> protons appear at 8.7, 4.3, and 2.0 ppm, respectively. The -SH proton resonance is part of the 2.0 ppm peak. <sup>1</sup>H MAS NMR spectrum of <sup>13</sup>C-CysAu is shown in the bottom spectrum along with peak assignments. The broad resonances centered at 7.6 ppm, 4.3 ppm and 2.0 ppm are from the -NH<sub>3</sub><sup>+</sup>, -CH, and -CH<sub>2</sub> groups, respectively. The sharp <sup>1</sup>H resonances at 2.1 ppm and 2.5 ppm are from the -CH<sub>2</sub> protons. The sharp <sup>1</sup>H resonance at 1.9 ppm is from the -SH protons, and the sharp resonance at 5.5 ppm is from water. Sixteen and 385 transients were obtained for the <sup>13</sup>C-Cys and <sup>13</sup>C-CysAu spectra at MAS speeds of 60 and 53 kHz, respectively.

were 0.76 μs and 1.0 μs, respectively. A recycle delay of 6 s was used for both <sup>1</sup>H and {<sup>1</sup>H}<sup>13</sup>C (CP) HETCOR (Heteronuclear Correlation) experiments. The <sup>1</sup>H-<sup>13</sup>C cross-polarization (CP) time for the {<sup>1</sup>H}<sup>13</sup>C (CP) HETCOR experiment was set to 400 μs in order to correlate (proton-carbon) only with the

closest protons. Frequency switched Lee–Goldburg (FSLG) decoupling<sup>18</sup> was used on the proton channel during the  $t_1$  ( $^1\text{H}$ ) evolution time and heteronuclear TPPM decoupling was used on the  $^{13}\text{C}$  channel during the data acquisition time.<sup>19</sup>

## RESULTS AND DISCUSSION

**$^1\text{H}$  and  $^2\text{H}$  MAS NMR Spectroscopy of  $^2\text{H}$ -Cys.** The  $^1\text{H}$  resonance of the thiol proton was not uniquely identifiable in the spectrum of  $^{13}\text{C}$ -Cys (see Figure 2). Since the two-layer model for cysteine-coated gold nanoparticles suggested that thiol protons would be present in the outer layer, it was deemed important to clearly determine where thiol protons would contribute in the  $^1\text{H}$  MAS NMR spectrum. Consequently,  $^2\text{H}$ -Cys was examined with the assumption that the  $\text{C}_3$  protons and thiol protons have  $^1\text{H}$  NMR resonances that either overlap or are very close to one another. Deuteration of the  $\text{C}_3$  carbon eliminated the contribution to the  $^1\text{H}$  spectrum of the  $\text{C}_3$  protons.  $^2\text{H}$ -Cys was recrystallized from  $\text{D}_2\text{O}$  that had a small amount (nonstoichiometric drop) of  $\text{HCl}$ ; consequently, the amino and thiol groups would at least be partially deuterated. The acquired  $^2\text{H}$  MAS NMR spectrum is shown in Figure 1 (top). An expansion of the centerband is shown in Figure 1 (middle) and clearly shows the presence of  $-\text{CD}_2$  and  $-\text{ND}_3^+$  deuterons. In addition, there is a less intense  $^2\text{H}$  resonance located where a hydroxyl deuteron would be expected to appear.

Crystalline cysteine occurs in several forms. When recrystallized from water, cysteine appears in the zwitterion form. However, hydroxyl protons are present when cysteine is recrystallized as an  $\text{HCl}$  salt. Hence, the small nonstoichiometric amount of added  $\text{HCl}$  during recrystallization produced a sample that contains crystals with zwitterions and other crystals (a smaller fraction) with cysteine molecules having hydroxyl groups. Since the deuterated sample was recrystallized from  $\text{D}_2\text{O}$ , it was expected that the thiol groups would be at least partially deuterated. The expected deuterium resonance of the thiol deuteron is not clearly identifiable in the  $^2\text{H}$  spectrum, but it may overlap with the  $-\text{CD}_2$  deuterium resonance.

Intense peaks from  $-\text{CH}$ ,  $-\text{NH}_3^+$ , and  $-\text{SH}$  protons appeared in the  $^1\text{H}$  spectrum of  $^2\text{H}$ -Cys (Figure 1, bottom). A less intense peak appeared at 19 ppm, consistent with contributions from hydroxyl protons. The sought after  $^1\text{H}$  resonance from the thiol proton became evident because the  $-\text{CH}_2$  protons were replaced with deuterons in the starting material. The thiol proton resonance appears at 1.9 ppm in the  $^1\text{H}$  spectrum and makes a contribution to the  $^1\text{H}$  spectrum comparable to that made by  $\text{C}_2$  protons.

**$^1\text{H}$  MAS NMR Spectroscopy of  $^{13}\text{C}$ -Cys and  $^{13}\text{C}$ -CysAu.** The  $^1\text{H}$  MAS NMR spectrum of  $^{13}\text{C}$ -Cys shown in Figure 2 (top) is dominated by three broad resonances. The peak at 8.7 ppm is from the amino protons and the peak at 4.3 ppm is from  $\text{C}_2$  protons. The  $\text{C}_3$  protons contribute to the peak centered at 2.0 ppm. A distinct  $^1\text{H}$  resonance from thiol protons is not readily discernible in the spectrum, as addressed earlier, but is part of the broad peak shared with the  $\text{C}_3$  protons.

The  $^1\text{H}$  spectrum of  $^{13}\text{C}$ -CysAu, obtained by a simple  $90^\circ$  – acquire pulse sequence, is shown in Figure 2 (bottom). It is evident that two sets of  $^1\text{H}$  resonances are present. The broad resonances are greater in width to those observed in  $^{13}\text{C}$ -Cys (top spectrum). Approximate  $^1\text{H}$  linewidths for the various samples are shown in Table 1. The broad feature at 7.6 ppm is from amino protons and the broad feature at 4.3 ppm is from  $\text{C}_2$  protons. The broad feature centered at 2 ppm (under the

**Table 1. Approximate Full-Width-Half-Maximum Values of  $^1\text{H}$  Resonances, in Hz**

sample\functional group	$-\text{NH}_3^+$	$-\text{CH}$	$-\text{CH}_2$	$-\text{SH}$	$\text{H}_2\text{O}$
$^{13}\text{C}$ -Cys	800	1000	630		
$^{13}\text{C}$ -CysAu (broad)	1960	2000			
$^{13}\text{C}$ -CysAu (sharp)			70	100	80

sharp resonances) is assigned to  $\text{C}_3$  protons. The sharp set of resonances observed in the  $^1\text{H}$  spectrum of  $^{13}\text{C}$ -CysAu have linewidths an order of magnitude smaller than the proton resonances observed in  $^{13}\text{C}$ -Cys (see Table 1). The pair of intense sharp peaks at 2.1 ppm and 2.5 ppm (frequency difference of 200 Hz) is assigned to the  $\text{C}_3$  protons. The  $\text{C}_3$  protons are directly bonded to a  $^{13}\text{C}$  nucleus (only the  $\text{C}_3$  carbon is  $^{13}\text{C}$  labeled), and a solution  $^1\text{H}$  NMR spectrum (see Figure S1 in the Supporting Information) showed a  $^1\text{H}$ – $^{13}\text{C}$  scalar coupling of 144 Hz between the  $\text{C}_3$  protons and the  $^{13}\text{C}$  spin at the  $\text{C}_3$  carbon position. Accordingly, this pair of peaks is the result of the  $^1\text{H}$ – $^{13}\text{C}$  scalar coupling and is assigned to the  $\text{C}_3$  protons. The sharp peak at 1.9 ppm is from thiol protons; this assignment is supported by the  $^1\text{H}$  spectrum of  $^2\text{H}$ -Cys in Figure 1. The contribution of the thiol protons to the  $^1\text{H}$  spectrum provides strong support for the cysteine bilayer model. The intensity of the contribution made by thiol protons to the  $^1\text{H}$  NMR spectrum (assumed to made of the features at 1.9 ppm and lower) is approximately half the intensity contributed by the two sharp  $\text{C}_3$  proton resonances. This 1:2 ratio of signal intensities is consistent with two  $-\text{CH}_2$  protons contributing to the spectrum for every one  $-\text{SH}$  proton. Hence, the set of sharp resonances is from cysteine molecules forming the outer layer of the bilayer system since only that layer can have thiol protons. The absence of a  $^1\text{H}$  resonance in the region of the spectrum where hydroxyl protons would contribute (around 19 ppm) indicates that cysteine molecules in the gold nanoparticle system exist in the zwitterion form, which has rich hydrogen bonding possibilities.

The sharp peak at 5.5 ppm is assigned to water. The position of the peak is consistent with a  $^1\text{H}$  NMR signal coming from water. Two additional  $^1\text{H}$  NMR spectra (Figures S2 and S3 shown in the Supporting Information) were taken about one year after the original data was taken on  $^{13}\text{C}$ -CysAu to support the assignment of the peak at 5.5 ppm to water. Figure S2 shows the  $^1\text{H}$  spectrum of the sample after spending one year in a sealed bottle that was also placed in a zip lock bag. The sharp  $^1\text{H}$  resonance at 5.5 ppm is still present. After the spectrum in Figure S2 was acquired, the sample was removed from the spectrometer and exposed to deuterated water vapor for two days. A  $^1\text{H}$  spectrum was obtained after the exposure and is shown in Figure S3. The intense sharp peak at 5.5 ppm in Figure S2 is no longer present in Figure S3. This is strong evidence that water molecules are the source of the sharp resonance at 5.5 ppm.

A natural question is why don't the  $-\text{CH}$  protons have a sharp  $^1\text{H}$  resonance feature. Cysteine molecules in the inner layer are rigidly held in place, being anchored to the gold surface at the sulfur end and tied down via hydrogen bonding at the amino/carboxylate end of the molecule. The environment of the molecules in the outer layer is not as restrictive. The amino/carboxylate groups of these molecules are hydrogen bonded to the inner layer. However, the sulfur end of the molecule is free to explore a more open space. Hence, large amplitude motions about the  $\text{S}-\text{C}_3$  and the  $\text{C}_3-\text{C}_2$  bonds are



possible, but such motions about the  $C_1$ – $C_2$  and  $N$ – $C_2$  bonds are prohibited. Consequently, the  $-CH_2$  and  $-SH$  protons may undergo large amplitude motional averaging leading to their sharper resonances whereas motional averaging of the  $-CH$  proton does not occur and results in only a broad resonance feature. Figure 3 shows a model that is being proposed which

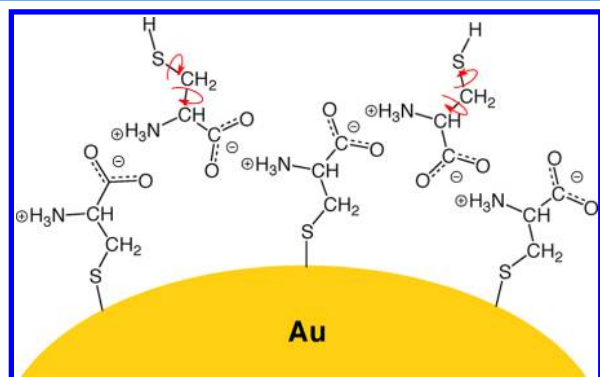


**Figure 3.** Bilayer model of cysteine on gold. Bonds capable of large amplitude motions are marked with arrows.

illustrates some of the details just discussed. The arrows around the  $S$ – $C_3$  and  $C_3$ – $C_2$  bonds of the cysteine molecules in the outer layer represent large amplitude motions about those bonds.

**$\{^1H\}^{13}C$  HETCOR MAS NMR of  $^{13}C$ -CysAu.** The  $\{^1H\}^{13}C$  CP HETCOR MAS NMR<sup>20</sup> spectrum of  $^{13}C$ -CysAu in Figure 4 shows the presence of two spectroscopically different  $C_3$  carbons, labeled  $C_3^*$  and  $C_3$ . According to previously published results, the deshielded feature,  $C_3^*$ , comes from cysteine molecules chemisorbed to the gold surface, and the feature labeled  $C_3$  is from cysteine molecules that form an outer layer to the chemisorbed layer. The  $C_3$  protons dominate the

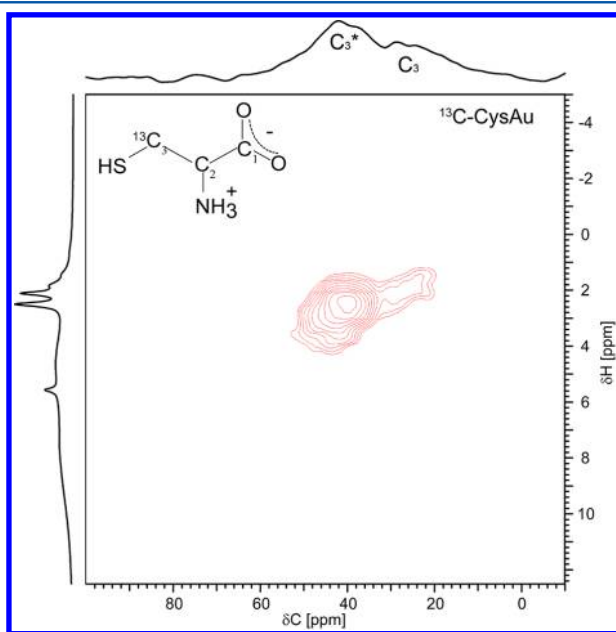


**Figure 4.**  $\{^1H\}^{13}C$  HETCOR (CP) MAS NMR spectrum of  $^{13}C$ -CysAu. For reference, the proton spectrum of  $^{13}C$ -CysAu shown in Figure 2 is displayed along the  $^1H$  axis of the HETCOR spectrum. 128 transients, 64 t1 points and a MAS speed of 53 kHz were used for the HETCOR experiment.

HETCOR spectrum because of the short  $^1H$ – $^{13}C$  cross-polarization contact time and their proximity to the  $^{13}C$  label. The asymmetric dumbbell shaped contour spectrum shows two different populations of  $C_3$  protons are present, which suggests that there are two different types of cysteine molecules contributing to the spectrum. The projections of the centers of the large and small lobes onto the  $^1H$  axis are around 2.5 ppm and 2.0 ppm, respectively. The deshielded large lobe at 2.5 ppm is associated with the chemisorbed  $C_3^*$  feature, and the smaller lobe at 2.0 ppm belongs to the  $C_3$  feature. The deshielded  $^{13}C$  and deshielded  $^1H$  NMR resonances are associated with chemisorbed molecules of cysteine.

The ratio of the intensity of the  $^{13}C$  NMR signals from the peaks labeled  $C_3^*$  and  $C_3$  is approximately 1.8. The lower intensity of the signal from the  $C_3$  carbon (outer layer) may arise from less efficient  $^1H$ – $^{13}C$  cross-polarization because of the motional averaging of the outer layer mentioned in the previous section.

## CONCLUSIONS

The  $^1H$ ,  $^2H$  and  $\{^1H\}^{13}C$  (CP) HETCOR MAS NMR experiments provide evidence that L-cysteine forms two layers on gold nanoparticles. The  $\{^1H\}^{13}C$  (CP) HETCOR and  $^1H$  NMR data show that two types of cysteine are present in  $^{13}C$ -CysAu, as is evidenced by the double lobed HETCOR spectrum in Figure 4 and the presence of broad and sharp resonances in the proton spectrum in Figure 2. Furthermore, the  $^1H$  MAS NMR spectrum of  $^{13}C$ -CysAu clearly shows the presence of a thiol proton and has no contribution from hydroxyl protons. Together, the data support the picture of cysteine zwitterions forming a two-layer coverage of the gold nanoparticles. An inner layer is chemisorbed to the gold surface via the sulfur atom, and a second layer is hydrogen bonded to the chemisorbed layer. The sharp set of proton resonances observed for the  $-CH_2$  and  $-SH$  protons of  $^{13}C$ -CysAu and the lack of sharp resonances of the  $-CH$  proton in the sample are indicative of large amplitude motions about the  $S$ – $C_3$  and  $C_3$ – $C_2$  bonds for cysteine in the outer layer.

Because of the expense associated with using  $^{13}C$  and  $^{15}N$  labeled cysteine in an earlier study<sup>17</sup> and  $^{13}C$  labeled cysteine in this work, it was not possible to study the structure of cysteine on gold as a function of pH during sample preparation. This work shows a signature for the formation of a bilayer of cysteine is the presence of sharp  $^1H$  resonances for the  $-CH_2$  and  $-SH$  protons. Hence, high speed  $^1H$  MAS NMR may provide an inexpensive way to determine the number of cysteine layers on gold nanoparticles as a function of pH since isotopically labeled samples would not be required.

## ASSOCIATED CONTENT

### Supporting Information

Solution state  $^{13}C$  spectra of  $^{13}C$ -Cys (Figure S1).  $^1H$  MAS spectrum taken on  $^{13}C$ -CysAu approximately 6 months after the spectrum in Figure 2 was taken (Figure S2).  $^1H$  MAS spectrum taken on  $^{13}C$ -CysAu after being exposed for 2 days to a vapor of deuterated water (Figure S3). This material is available free of charge via the Internet at <http://pubs.acs.org>.

## AUTHOR INFORMATION

### Notes

The authors declare no competing financial interest.

## ■ ACKNOWLEDGMENTS

This work was supported by Grant CHE-0846583 from the National Science Foundation. We thank Dr. Novruz Akhmedov for taking solution spectra during the course of this work.

## ■ REFERENCES

- (1) Kuhnle, A. *Curr. Opin. Colloid Interface Sci.* **2009**, *14*, 157.
- (2) Sasaki, Y. C.; Yasuda, K.; Suzuki, Y.; Ishibashi, T.; Satoh, I.; Fujiki, Y.; Ishiwata, S. *Biophys. J.* **1997**, *72*, 1842.
- (3) Renzi, V.; Lavagnino, L.; Corradini, V.; Biagi, R.; Cnepe, M.; Pennino, U. *J. Phys. Chem. C* **2008**, *112*, 14439.
- (4) Kuhnle, A.; Molina, L. M.; Linderroth, T. R.; Hammer, B.; Besenbacher, F. *Phys. Rev. Lett.* **2004**, *93*, 086101.
- (5) Kuhnle, A.; Linderroth, T. R.; Schunack, M.; Besenbacher, F. *Langmuir* **2006**, *22*, 2156.
- (6) Kuhnle, A.; Linderroth, T. R.; Hammer, B.; Besenbacher, F. *Nature* **2002**, *415*, 891.
- (7) Callaro, A.; Terreni, S.; Caballeri, O.; Prato, M.; Cvetko, D.; Morgante, A.; Floreano, L.; Canepa, M. *Langmuir* **2006**, *22*, 11193.
- (8) Canepa, M.; Lavagnino, L.; Pasquali, L.; Moroni, R.; Bisio, F.; Renzi, V.; Terreni, S.; Mattera, L. *J. Phys.: Condens. Matter* **2009**, *21*, 1.
- (9) Shin, T.; Kim, K.-N.; Lee, C.-W.; Shin, S. K.; Kang, H. *J. Phys. Chem. B* **2003**, *107*, 11674.
- (10) Uvdal, K.; Bodo, P.; Liedberg, B. *J. Colloid Interface Sci.* **1992**, *149*, 162.
- (11) Nazmutdinov, R. R.; Zhang, J.; Zinkicheva, T. T.; Manyurov, I. R.; Ulstrup, J. *Langmuir* **2006**, *22*, 7556.
- (12) Caballeri, O.; Oliveri, L.; Dacca, A.; Parodi, R.; Rolandi, R. *Appl. Surf. Sci.* **2001**, *175*, 357.
- (13) Doderio, G.; Michieli, L. D.; Cavalleri, O.; Rolandi, R.; Oliveri, L.; Dacca, A.; Parodi, R. *Colloids Surf. A* **2000**, *175*, 121.
- (14) Dakkouri, A. S.; Kolb, D. M.; Edelstein-Shima, R.; Mandler, D. *Langmuir* **1996**, *12*, 2849.
- (15) Xu, Q.-M.; Wan, L.-J.; Wang, C.; Bai, C.-L.; Wang, Z.-Y.; Nozawa, T. *Langmuir* **2001**, *17*, 6203.
- (16) Zhang, J.; Chi, Q.; Nielsen, J. U.; Friis, E. P.; Andersen, J. E. T.; Ulstrup, J. *Langmuir* **2000**, *16*, 7229.
- (17) Abraham, A.; Mihaliuk, E.; Kumar, B.; Legleiter, J.; Gullion, T. J. *Phys. Chem. C* **2010**, *114*, 18109.
- (18) Bielecki, A.; Kolbert, A. C.; Levitt, M. H. *Chem. Phys. Lett.* **1989**, *155*, 341.
- (19) Bennett, A. E.; Rienstra, C. M.; Auger, M.; Lakshmi, K. V.; Griffin, R. G. *J. Chem. Phys.* **1995**, *103*, 6951.
- (20) Vega, A. J. *J. Am. Chem. Soc.* **1988**, *110*, 1049.